Published in final edited form as:
Int J Appl Earth Obs Geoinf. 2020 April ; 86: 102027. doi:10.1016/j.jag.2019.102027.

Estimation of leaf area index using PROSAIL based LUT inversion, MLRA-GPR and empirical models: Case study of tropical deciduous forest plantation, North India

Sanjiv K. Sinha[a], **Hitendra Padalia**[a,*], **Anindita Dasgupta**[a], **Jochem Verrelst**[b], **Juan Pablo Rivera**[c]

Sanjiv K. Sinha: s.sanjivevs@gmail.com; Anindita Dasgupta: anindita.ces@gmail.com; Jochem Verrelst: Jochem.verrelst@uv.es; Juan Pablo Rivera: juan.rivera@uv.es, jprivera@conacyt.mx

[a]Indian Institute of Remote Sensing, Indian Space Research Organisation (ISRO), 4-Kalidas Road, Dehradun, 248001, Uttarakhand, India

[b]Image Processing Laboratory (IPL), Parc Científic, Universitat de Valéncia, 46980 Paterna, Valéncia, Spain

[c]Conacyt-UAN-CENiT2 Centro Nayarita de Innovación y transferencia de tecnologia, Calle 3 esquina con Av. 9 /n colonia Ciudad Industrial, 63173 Tepic, Nayarit, Mexico

Abstract

Forests play a vital role in biological cycles and environmental regulation. To understand the key processes of forest canopies (e.g., photosynthesis, respiration and transpiration), reliable and accurate information on spatial variability of Leaf Area Index (LAI), and its seasonal dynamics is essential. In the present study, we assessed the performance of biophysical parameter (LAI) retrieval methods *viz*. Look-Up Table (LUT)-inversion, MLRA-GPR (Machine Learning Regression Algorithm-Gaussian Processes Regression) and empirical models, for estimating the LAI of tropical deciduous plantation using ARTMO (Automated Radiative Transfer Models Operator) tool and Sentinel-2 satellite images. The study was conducted in Central Tarai Forest

*Corresponding author. hitendra@iirs.gov.in (H. Padalia).

Authors statement

I/We have submitted a revised manuscript entitled “Estimation of Leaf Area Index using PROSAIL based LUT Inversion, MLRA-GPR and Empirical Models: Case Study of Tropical Deciduous Forest Plantation, North India” for consideration as a research article by the International Journal of Applied Earth Observation and Geoinformation.

I/We attempt to address all queries of the reviewers and revised our manuscript as suggested by reviewers. Thank you for your consideration of this manuscript.

Dr. Hitendra Padalia

Respected sir,

Sincerely,

Declaration of Competing Interest

Respected sir,

All persons who meet authorship criteria mentioned as authors, and on the behalf of all authors certify that they have participated sufficiently in the work to take public responsibility for the content, including participation in the concept, design, analysis, writing, or revision of the manuscript. Furthermore, I/We confirm that this work is original and has not been published elsewhere nor is it currently under consideration for publication elsewhere.

Thank you for your consideration of this manuscript.

Sincerely,

Hitendra Padalia

Europe PMC Funders Author Manuscripts

Division, Haldwani, located in the Uttarakhand state, India. A total of 49 ESUs (Elementary Sampling Unit) of 30m×30m size were established based on variability in composition and age of plantation stands. In-situ LAI was recorded using plant canopy imager during the leaf growing, peak and senescence seasons. The PROSAIL model was calibrated with site-specific biophysical and biochemical parameters before used to the predicted LAI. The plantation LAI was also predicted by an empirical approach using optimally chosen Sentinel-2 vegetation indices. In addition, Sentinel-2 and MODIS LAI products were evaluated with respect to LAI measurements. MLRA-GPR offered best results for predicting LAI of leaf growing (R^2 = 0.9, RMSE = 0.14), peak (R^2 = 0.87, RMSE = 0.21) and senescence (R^2 = 0.86, RMSE = 0.31) seasons while LUT inverted model outperformed VI's based parametric regression model. Vegetation indices (VIs) derived from 740 nm, 783 nm and 2190 nm band combinations of Sentinel-2 offered the best prediction of LAI.

Keywords

Leaf area index; Vegetation indices; Radiative transfer model Sentinel-2

1 Introduction

Knowledge of leaf area of vegetation canopies is crucial for understanding its interaction with the prevailing climate (Bright et al., 2015). The leaf area interacts with solar radiation to produce energy by regulating canopy gaseous exchanges. It, therefore, regulates photosynthetic capability, stress, the productivity of the vegetation (Boegh et al., 2013). Leaf area is defined in the form of an index; called leaf area index (LAI). LAI is the half of total green leaves area per unit ground surface area and it is a dimensionless measure (Watson, 1947). The field-based LAI measurements using destructive sampling (Pérez-Harguindeguy et al., 2013) or non-destructive sampling (using plant canopy imagers such as LAI-2000, CI-110, Hemi-view, etc. based on gap fraction (Woodgate et al., 2015), though are precise, yet are not practical for systematic studies over extensive areas.

Satellite remote sensing data offer a synoptic coverage of the study area over time and thus enable the systematic observation of canopy conditions (Wulder et al., 2012). Since the past five decades, various remote sensing satellites including optical, microwave and LiDAR have been launched. Especially optical satellite data have been extensively used for vegetation studies from local to global scales. Satellite-based monitoring of forests is capable of capturing intra- and inter-annual canopy cover changes including LAI changes, and are increasingly used owing to their global coverage, repeated measurements, and easy availability (Liu et al., 2015). Several global LAI products have available with different optical sensors (NOAA/AVHRR (Nemani et al., 2009), SPOT/VEGETATION (Baret et al., 2007), Terra AQUA/MODIS (Yang et al., 2006), etc.). Global LAI products are available with courser resolution and do not capture the local variation of vegetation, topography, and soil, etc. It is essential for studying the vegetation processes to derive LAI information incorporating site-specific characteristics of vegetation. Sentinel 2A and 2B satellites, launched in the year 2015, offer high spatial, spectral and radiometric resolution images

and enhance the accuracy for retrieval of LAI at plot level in the forest (Clevers et al., 2017; Immitzer et al., 2016).

Over past three decades, extensive work has been done to establish robust LAI estimation techniques using radiative transfer theory for various ecosystems (e.g. forests, agriculture, and grasslands, etc) (Yang et al., 2011; Sehgal et al., 2016; Si et al., 2012). LAI plays an important role in multiple scattering within the canopy and in regulating the transmission of radiation. RTM is used for simulating canopy reflectance. RTMs can also be inverted against optical (reflectance) measurements to retrieve LAI. Anderson and Spiegel (1972)) and Ross (1981) applied the radiative transfer theory for measuring canopy parameters. Researchers have used inversion of Beer-Lambert Law to estimate LAI of the forests using measured transmittance and extinction coefficient (Monsi and Saeki, 1953). Jacquemoud and Baret (1990) developed PROSPECT (PROpriétésSPECTrales) to describe multi-directional reflectance and diffusion on the leaf level.

PROSPECT requires inputs on leaf biochemical (chlorophyll content) and structural parameters (complexity of the leaf structure) (Feret et al., 2008). The leaf model can be combined with other canopy models (e.g. SAIL) to describe the reflectance of the whole canopy, named PROSAIL (Jacquemoud et al., 2009). SAIL (Scattering by Arbitrarily Inclined Leaves) is a canopy reflectance model that takes into account the dependence of canopy reflectance on the structural and optical parameters of the canopy. Key components that are used in the SAIL model are information about leaves, soil background, sun-illumination, view geometries and interaction of radiation within the canopy (Goel and Thompson, 2000). These components were selected on the basis of sensitivity analysis. Sensitivity analysis is used to find the key variables driving the model (Verrelst et al., 2015b). In the recent study by (Li et al., 2017), canopy reflectance was modeled using PROSAIL for three types of subtropical forests in China. (Wu et al., 2017) used Canopy RTM, PROSAIL along with satellite-observed seasonal patterns while studying Amazon evergreen forest. Verrelst et al. (2015a) give information on the available LAI retrieval methods and techniques that have been applied to the scientific software package ARTMO (Automated Radiative Transfer Model Operator).

ARTMO brings leaf and canopy models at one platform and provides tools for LAI retrieval. Furthermore, spatial LAI can be obtained following three main retrieval approaches: (i) by developing a statistical relationship through parametric regression between LAI and vegetation indices (VIs), (ii) data-driven relationships through machine learningbased regression (MLRA), and (iii) through physically-based inversion of a RTM, e.g. by means of Look-Up Tables (LUT) (Verrelst et al., 2018). Parametric regression methods involve derivation of the statistical relationship between a parameter of interest, and suitable channels of satellite image and using the regression models for spatial prediction of the parameter. VIs are most commonly used, and make use of various spectral bands in deriving relationship with LAI (Delegido et al., 2015).

Parametric regression techniques are used to establish a relationship between the variable (e.g., in-situ measured LAI) and remote sensing image derived VIs (Verrelst et al., 2018). Researchers have studied the sensitivity of various VIs such as NDVI (Normalized

Difference Vegetation Index), Normalized Difference Index (NDI), EVI (Enhanced Vegetation Index) and other indices towards in-situ measured LAI (Huete et al., 2002; Delegido et al., 2011; Croft et al., 2014; George et al., 2018; Padalia et al., 2019) using empirical approaches. The empirical approach is straightforward and often yields good results. However, the statistical relationships between in-situ LAI and satellite-derived VIs may vary with the satellite sensor, site and sampling condition (Zhou et al., 2014; Yang et al., 2016; Wu et al., 2017; Lu et al., 2018).

Machine learning regression algorithms (MLRA) are a family of non-parametric methods such as Gaussian processes regression (GPR), Neural Networking (NN), Genetic Algorithm and Support Vector Machine (SVM) and Kernel Ridge Regression (KRR)) to predict bio-physical parameter (Verrelst et al., 2018). Machine learning techniques rely on non-linear equations on which models are built. GPR method has been found best with the simulated Sentinel-2 data for predicting crop LAI (Verrelst et al., 2015c). GPR has some advantages over other MLRAs such as it needs fewer sample points, provides predictive mean as well predictive variance and maximizing the marginal likelihood in the training set which is learned by hyperparameters by appropriate kernel function (Rasmussen and Williams, 2006).

Physically-based inversion (i.e. LUT-inversion) of an RTM approach is based on physical laws and works on the principle of cause and effect that can be used for developing physical models to estimate LAI based on canopy reflectance (Houborg et al., 2007). LUT-inversion retrieval techniques linking the spectral fitting of simulated spectra to the appropriate measured LAI value (i.e. LUT) through a defined mathematical algorithm (i.e. cost function) (Rivera et al., 2013). LUT-inversion allows choosing the best wavelength and cost-function to minimize residual for spectral fitting (Verrelst et al., 2015a). Moreover, it takes minimum computation time than other retrieval techniques (Dorigo et al., 2007).

This study aims to evaluate the capabilities of different retrieving tools *viz.* VIs, MLRA, and LUT-inversion, from ARTMO and PROSAIL Model for estimation of LAI of tropical broadleaved forest plantation stand located in the Indo-Gangetic Plain of India. First, the PROSAIL model has been calibrated and validated with site-specific parameters and subsequently its comparison has been made with MLRA-GPR and VIs based LAI estimation methods using Sentinel-2 data. In addition, the PROSAIL and VI-derived LAI outputs have been compared with LAI products of MODIS and Sentinel-2.

2 Data and modeling

2.1 Study area

The study was carried out in the Bhakra forest range of the Tarai Central Forest Division, Haldwani located in the Uttarakhand state of India. The study area falls between 29°05′30″ N -29°15′50″ N latitude and 79°20′30″ E -79°28′40″ E longitude (Fig. 1). The study area is part of Indo-Gangetic Plain with gentle sloping physiography. The average altitude is 285 m AMSL. The climatic is a sub-humid monsoon. The mean temperature varies from 22 °C to 26 °C. The summers are very hot with temperatures often exceeding 40 °C during

Europe PMC Funders Author Manuscripts

the daytime in summer. The temperature drops below 5 °C during winters, where frost is common.

The area receives rainfall from southwest monsoon with maximum rains during July and August months. Average rainfall in the region has been 2076 mm/year (Shukla and Bora, 2003). The soil is alluvium loam with a well-developed soil profile. The native plantations of species such as *Holoptelea integrifolia* (Kanju), *Acacia catechu* (Khair), *Cassia fistula* (Amaltas), *Dalbergia sissoo* (Sisham), *Mallotus philippensis* (Rohini) are present in the study area. The average age of plantation is 10–15 years.

2.2 Field sampling design and LAI measurements

The criteria and terminologies of Land Product Validation (LPV) of the Committee of Earth Observation Satellites (CEOS) were followed in the field sampling design (Fig. 2). An area of 7.5 km × 7.5km was chosen and plantations were stratified based on species and age. A total of 49 Elementary Sampling Units (ESUs) were laid out. Each ESU was 30m × 30m in size encompassing three fixed pattern Secondary Sampling Units (SSUs) of 5m × 5m were laid out along the diagonal axis of ESU. LAI was recorded within the well-marked SSUs within one week before and after sentinel-2 satellite pass from the study area during leaf growing(May), peak (October) and senescence (December) seasons using plant canopy analyzer.

Thus for each ESU, three hemispherical photographs were collected. LAI value from each hemispherical photograph was computed by applying appropriate sky and leaf filters in Plant Canopy Analysis System software. For each ESU, LAI values of three SSUs were averaged and the mean LAI value per ESU was obtained.

2.3 Sentinel-2 data and pre-processing

Sentinel-2 A was launched in 2015 as part of the Copernicus program of the European Space Agency (European Space Agency, 2015). It consists of two identical satellites, Sentinel-2A, and Sentinel-2B with 13 spectral bands, with a spatial resolution of 10 m, 20 m, and 60 m. The field of view is 290mm and revisit time is every five days under the same viewing angle. Open data policy adopted for the Copernicus program provides free access for the Sentinel data products at Sentinel scientific hub (European Space Agency, 2016a). Three sentinel-2 scenes belonging to 17th May 2018, 14th October 2017 and 8th December 2017 representing leaf growing, peak and senescence phases were downloaded. Sen2Cor Level-2A processor was used to correct single-date Sentinel-2 Level-1C products (digital number image) for the atmospheric effects and generating Level-2A surface reflectance product using SNAP (Sentinel Application Platform) Toolbox (European Space Agency, 2016b,c). Level-2A processing was applied to Level-1C orthoimage reflectance products to calculate reflectance using top-of-atmo-spheric correction. Processing involves the retrieval of aerosol optical thickness and the water vapor content from the L1C image (Main-Knorn et al., 2017).

Europe PMC Funders Author Manuscripts

2.4 LAI estimation using LUT inversion

2.4.1 PROSAIL parameterization—The ARTMO tool was downloaded from the web link: http://artmotoolbox.com. The PROSAIL model was parameterized based on the available value ranges of the respective biochemical and biophysical variables of the leaf as well as geometrical parameters (solar zenith angle, view azimuth angle and view observer angle) obtained from the field (Table 1).

Leaf samples of different species (*Holoptelia integrifolia*, *Acacia catechu*, *Cassia* fi*stula*, *Dalbergia sissoo*, *Mallotus philippensis*) were sampled for determining leaf dry matter content, leaf chlorophyll content and equivalent water thickness. The leaf samples were oven-dried and weighted to determine leaf dry matter content. The leaf water content was obtained by subtracting leaf fresh mass and leaf dry mass by the leaf area. The leaf chlorophyll content was computed using the acetone extraction method (Arnon, 1949). Leaf structural parameter (N) refers to the internal structure of the leaf. In monocots with compact mesophyll, N ranges from 1 to 1.5, dicots having spongy parenchyma, and the N value ranges between 1.5–2.5 (Jacquemoud, 1993). LAI value range was determined following method as described in section 2.2. Hotspot (m/m) is a proportion of average leaf size and the height of canopy (0.01: small leaves, tall canopies; 0.5: large leaves, short canopies) (Vuolo et al., 2005). For lower LAI values, sensitivity to background reflectance is maximum (Jacquemoud et al., 1996). Leaf angle refers to the orientation of leaves within the canopy (Bio-Science, 2011). Image of plant canopy imager (CI-110) was taken with top of the image-oriented to the north which corresponds to 0° for the azimuth angle. The solar zenith angle ranges between 0–90. Spitters (1986) worked on diffuse light and its implications on canopy photosynthesis. The values and ranges of few parameters (Leaf structural index (N), Soil brightness coefficient and Hot spot parameter) were obtained from the literature (Jacquemoud, 1993; Darvishzadeh et al., 2008b; Baret et al., 2010).

2.4.2 LUT inversion—According to Weiss et al. (2000) retrieving the accuracy of the model depends on the size of LUT. Therefore, various iteration (> 100,000) increases the accuracy of LAI estimation. Primarily LUT was generated with 100,000 sets of parameters with the help of a user-defined range of value for each parameter (Eq. 1). PROSAIL model uses these combinations of input parameters for the forward run to simulates canopy reflectance. Simulated canopy reflectance was synchronizing with the Sentinel-2 reflectance for model inversion (i.e. LUT-inversion). A cost function (e.g. root mean square error (RMSE)) (Eq. 2) was used to find the best fitting simulated spectra to measured reflectance spectra through LUT for corresponding LAI value. The overall time taken by inversion was 190 s. for inversion and 75 min for image generation in MATLAB version R2017a on a 64 bit Windows 8 platform.

$$F(n) = a-(b-a)x\ \mathrm{rand}(n) \quad (1)$$

Where, F, a and b are variable, higher and lower value of the variables, respectively, and n is a number of iterations to generate LUT.

$$\text{RMSE} = \sqrt{\sum_{i=0}^{n} \frac{(Rmeasured - Rsimulated)2}{(n)}} \quad (2)$$

Where, Rmeasured and Rsimulated are the LAI measured (*in-situ*) and LAI simulated by PROSAIL respectively.

2.4.3 Machine learning regression algorithm - gaussian processes regression (MLRA-GPR)—

Gaussian processes regression (GPR) is an efficient MLRA model for retrieving biophysical parameters (Caicedo et al., 2014). It is based on a Bayesian (probability) approach for learning generic regression kernels between input (remote sensing data) and the output variables (bio-physical parameter) (Verrelst et al., 2015a). GPR models are non-parametric as well non-linear while at the same time it provides a ranking of relevant bands (features) from input spectral data obtained from remote sensing.

2.5 LAI Estimation using a parametric regression model

2.5.1 Sentinel-2 VIs—

Four commonly used VIs, i.e., (1) Normalized Difference Vegetation Index (NDVI), (2) Normalized Difference Index (NDI), (3) Soil-adjusted Vegetation Index (SAVI) and (4) Non-linear Vegetation Index (NLI) were chosen for estimation of LAI using linear regression (Table 2).

2.5.2 Sensitivity analysis of VIs—

ARTMO's Spectral Indices (SI) Toolbox was used to derive various combinations of selected VIs. These VIs were tested for different functions such as linear, non-linear, polynomial and logarithmic with the Sentinel-2 spectral reflectance bands. 2-D correlation plots were used to determine the most sensitive wavebands and VIs to LAI of the plantation. The VIs offering the highest correlation with field-measured LAI was chosen for the prediction of LAI and validation.

2.5.3 Validation—

The efficiency of the models was assessed by the combination of RMSE and coefficient of determination (R^2) between the modeled and measured LAI. LAI outputs were validated by computing RMSE between measured and modeled LAI (RMSEr) as given in Eq. 3.

$$\text{RMSEr} = \sqrt{\frac{\sum_{i=1}^{n}(R_{measured} - R_{lut})^2}{n}} \quad (3)$$

where, $R_{measured}$ is the measured LAI and R_{lut} is the modeled LAI, and n is the number of ESUs.

3 Results

3.1 Seasonal LAI variation

Mean LAI values of 49 ESUs showed different seasonal variation patterns (Fig. 3). Lowest mean LAI (1.6 ± 0.69) was recorded during the leaf growing phase of May month. Maximum mean LAI (2.5 ± 0.74) values were recorded during the October month while moderate mean LAI (2.1 ± 0.67) values recorded during the early stage of leaf senescence

Europe PMC Funders Author Manuscripts

season i.e. December month. The LAI values varied significantly between measurement seasons ($P < 0.001$).

Among three seasons, LAI variation was higher (larger standard deviation) during the leaf growing season compared to peak and senescence season. The lowest variation was found in the peak LAI season. Field LAI values had symmetric distribution during May while October LAI values were right-skewed and December LAI values were left-skewed.

3.2 Performance of VI's based parametric regression model

2-D correlation plots revealed LAI sensitive wavebands and VIs of Sentinel-2. Wavebands located at 740 nm, 783 nm, 842 nm, 865 nm, and 2190 nm showed the highest sensitivity to LAI (Fig. 4).

Red edge bands (at 705 nm, 740 nm, and 783 nm) along with NIR bands (at 842 nm and 865 nm) showed a stronger correlation with SWIR bands (2190 nm). However, NDVI showed a good correlation with observed LAI (plots with > 90% canopy cover) during leaf growing (R^2-0.80, RMSE-0.18), peak (R^2-0.78, RMSE-0.22) and senescence (R^2-0.76, RMSE -0.23) seasons (Fig. 5).

3.3 Performance of non-parametric regression model (GPR)

As opposed to VI-based techniques, the GPR was found more stable with a low variance; therefore, render a higher prediction accuracy (Fig. 6). MLRA-GPR provided a better prediction of LAI in the three seasons as evident High R^2 values of 0.9, 0.87 and 0.86 were obtained for the month of May, October and December with an RMSE of 0.14, 0.21 and 0.31 respectively.

3.4 Performance of physically-based LUT inversion methods

LUT inversion (cost function least absolute error) method retrieved LAI with R^2 of 0.86 (RMSE -0.25), 0.87 (RMSE -0.19), and 0.86 (RMSE -0.21) in May, October, and December, respectively (Fig.7). Altogether, MLRA-GPR was found more stable among all retrieval methods with low variance and higher prediction accuracy.

MLRA-GPR provided a better prediction of LAI in the three seasons as evident high R^2 values of 0.9 with the lowest RMSE value (i.e. 0.14). However, for the month of October and December MLRA-GPR and LUT inversion provide the highest and equal R^2 i.e. 0.87 and 0.86 respectively. Though, LUT inversion provides the lowest RMSE value for the month of October and December than MLRA-GPR (Table 3).

Based on the lowest simulation time as well lowest RMSE value for two months with equal R^2 to best fit model, we have generated the LAI map through LUT Inversion methods for all three months (May, October, and December). The area with a dense growth of Kanju, Sisham, Khair and Rohini species showed higher LAI in peak growth season (i.e. October month) (Fig.8). The highest residual error was estimated for areas with lower LAI value than intermediate and lower LAI ranges. Lower residual error areas represent a close match between simulated LAI and field-measured LAI observations. The sparse vegetation, open spaces, and rivers are also represented by high residual errors.

3.5 Comparison with Global LAI products

The MODIS LAI algorithm is a function of the architecture of an individual tree canopy as a variable from vegetation land cover classes and spectral profile with a transmittance of vegetation variables. Leaf distribution inside canopy described by a 3-dimensional leaf area distribution factor (Knyazikhin et al., 1999).

Sentinel 2 LAI product is generated by linking reflectance from top of the canopy (TOC) estimated by PROSAIL to associated canopy architecture from its comprehensive database by neural networking (Weiss et al., 2016). SNAP Sentinel-2 LAI product grossly underestimated LAI of the study area in all seasons (R^2 of 0.55, 0.42, and 0.63 in the month of May, October, and December respectively (Fig. 9). MOD15 LAI product is widely used in various productivity models and phenology studies at the landscape level. To make comparable with different spatial resolution

data averaged all pixels of Sentinel-2 raster inside the single pixel of MOD15 LAI pixel (Wu et al., 2016). MODIS products even performed inferior to Sentinel-2 products in predicting LAI (R^2 of 0.46, 0.67, 0.31 in May, October and December respectively) of the study area.

4 Discussion

Model performances were evaluated for different leaf stages of tropical deciduous forest plantations. The RT theory-based LUT inversion model was calibrated with site-specific biophysical and biochemical parameters. The sensitivity of different bands of Sentinel-2 and commonly derived VIs to field measured LAI was investigated and the most sensitive spectral index was chosen for predicting LAI. The LUT and VIs based LAI outputs along with LAI products from MODIS and Sentinel-2 for were validated with independent LAI datasets.

4.1 Performance of LAI retrieval models

A comparative evaluation of three LAI estimation methods, namely: physically-based LUT inversion of RTM model, MLRA-GPR based non-parametric regression model and VIs based parametric regression model were performed. LUT inversion along with MLRA-GPR outperformed the parametric regression model with a higher coefficient of determination (R^2) (Table 3). MLRA-GPR outperformed LUT inversion for the month of May with higher R^2 and equal R^2 for the rest of two months. However, RMSE is higher than LUT inversion model due to LAI estimated by MLRA-GPR has the highest rage of value. Caicedo et al. (2014) found that GPR is the robust and best performing ML regression algorithms for LAI retrieval with R^2 0.94–0.99. However, Atzberger et al. (2015) found that RTM inversion with LUT predicts LAI accurately (R^2 = 0.91, RMSE = 0.18). Earlier studies found that LUT inversion performed better than spectral features based parametric regression model for grassland and boreal forest canopy (Gemmell et al., 2002; Darvishzadeh et al., 2008a). Based on our studies and previous results we selected the LUT inversion method for image generation as it takes less iteration time 190 s. for inversion and 75 min for image generation in respect to MLR-GPR as an unsuccessful attempt to image generation taking more than 5 h. with a system configures with 8 GB ram and i5 Intel processor. Operational LAI products

(Sentinel-2 and MODIS) provide a grossly underestimated LAI in different seasons. The structural complexity of tropical forest canopies and the use of some of the parameters from literature in the PROSAIL model might have affected the LAI retrieval accuracy in this study (Li et al., 2017).

4.2 LAI sensitive VIs

Delegido et al. (2011) and Padalia et al. (2019) observed that the Normalized Difference Index (NDI) derived from 705 nm and 665 nm band combination of Sentinel-2 show high sensitivity to LAI. However, in this study, VIs that used the Red and NIR portion of the spectra did not give a higher correlation with LAI as compared to the VIs constructed with SWIR and NIR bands. NDVI derived with the band combinations of NIR and SWIR wavelengths offered the best correlation with field-based LAI. Gong et al. (2003) also observed that band pairs the NIR and SWIR regions of the electromagnetic spectrum are most effective for LAI estimation. It is because NIR and SWIR bands are sensitive to leaf water content that in turn closely relates to LAI. Our findings correspond to Delegido et al. (2015), who observed that NDI formulated with a red edge band at 740 nm and the SWIR band at 2190 nm of Sentinel-2 data are best for estimation of LAI.

4.3 Effect of seasonal variation in LAI on model performance

LUT inversion based model was found best in predicting peak season LAI as compared to growing season and senescence season while parametric regression model was found best in predicting growing season LAI compared to peak season and senescence season. Whereas MLR-GPR was found best in predicting growing season i.e. May month. Studies have lower LAI value as a single layer deciduous canopy. Canopy cover shows heterogeneity in May and December month and homogeneity in October month with fully grown canopy. So that we are able to calibrate relationship with the low to moderate LAI value (~ 0–4). However, it will be helpful to study similar deciduous patches in foothills of Himalaya as well as tropical deciduous patches of central India (e.g. Vindhyan forest ranges) with low LAI value (Chaturvedi et al., 2017).

The plant canopy imagers recorded LAI observations were not corrected for clumping effects (Chianucci et al., 2015). Clumping effects cause underestimation of LAI values (Bao et al., 2018). We believe that the PROSAIL model prediction of LAI might have been further improved by providing a clumping effect corrected LAI range in the PROSAIL model. The satellite-based LAI prediction for the growing season might have also the effect of background undergrowth between plantation rows leading to the overestimation of LAI by the spectral indices and PROSAIL model.

5 Conclusion

The present study assessed the capabilities of PROSAIL-based LUT inversion, MLRA, and VIs for retrieval of LAI for tropical deciduous forest plantation using Sentinel-2 data. We calibrated PROSAIL based on site-specific parameters using ARTMO software and compared its performance with VIs based LAI estimation. Based on multi-season insitu LAI measurements, the accuracies and robustness of LAI estimation approaches were compared.

Europe PMC Funders Author Manuscripts

Results showed that the Non-parametric model along with the physically-based model performed better for retrieving LAI of forest plantation than VIs based parametric regression model. Among the various VIs tested, NDVI (band combinations of 740nm/783nm and 2190 nm) offered the most robust prediction of LAI. The seasonality of deciduous plantation was clearly observed to influence the performance of LAI retrieval methods, affecting LAI prediction accuracies. LAI retrieved through MLR-GPR model and LUT inversion model shows significantly higher accuracies compared to MOD15 and Sentinel-2 LAI products. Thus, findings emphasize the use of the PROSAIL model for generating regional-scale spatial LAI map through LUT inversion for further forest ecosystem related studies.

Acknowledgment

All authors would like to thank Dr. Prakash Chauhan, Director, and Dr. S. K Srivastav, Dean (A), Indian Institute of Remote Sensing for providing logistic facilities to execute this research. The authors also would like to thanks the Uttarakhand forest department, Haldwani for permission to collect field data in the study area.

References

Anderson JL, Spiegel EA. The moment method in relativistic radiative transfer. Astrophys J. 1972; 171: 127–138. DOI: 10.1086/151265

Arnon DI. Copper enzymes in isolated chloroplasts. Polyphenol Oxidase in Beta vulgaris. Plant Physiology. 1949. 1–15. [PubMed: 16654194]

Atzberger C, Darvishzadeh R, Immitzer M, Schlerf M, Skidmore A, le Maire G. Comparative analysis of different retrieval methods for mapping grassland leaf area index using airborne imaging spectroscopy. Int J Appl Earth Obs Geoinf. 2015; 43: 19–31. DOI: 10.1016/j.jag.2015.01.009

Bao Y, Ni W, Wang D, Yue C, He H, Verbeeck H. Effects of tree trunks on estimation of clumping index and LAI from hemiView and terrestrial LiDAR. Forests. 2018; 9: 1–16. DOI: 10.3390/f9030144

Baret F, de Solan B, Lopez-Lozano R, Ma K, Weiss M. GAI estimates of row crops from downward looking digital photos taken perpendicular to rows at 57.5° zenith angle: theoretical considerations based on 3D architecture models and application to wheat crops. Agric For Meteorol. 2010; 150: 1393–1401. DOI: 10.1016/j.agrformet.2010.04.011

Baret F, Guyou G. Potential and limitations of vegetation indices for LAI and APAR assessment. Remote Sens Environ. 1991; 35: 161–173.

Baret F, Hagolle O, Geiger B, Bicheron P, Miras B, Huc M, Berthelot B, Niao F, Weiss M, Samain O, Roujean J-L, et al. LAI, fAPAR and fCover CYCLOPES global products derived from VEGETATION: Part 1: Principles of the algorithm. Remote Sens Environ. 2007; 110: 275–286. DOI: 10.1016/j.rse.2007.02.018

Bio-Science. Plant Canopy Imager CI-110 Instruction Manual. 2011; 35

Boegh E, Houborg R, Bienkowski J, Braban CF, Dalgaard T, Van Dijk N, Dragosits U, Holmes E, Magliulo V, Schelde K, Di Tommasi P, et al. Remote sensing of LAI, chlorophyll and leaf nitrogen pools of crop- and grasslands in five European landscapes. Biogeosciences. 2013; 10: 6279–6307. DOI: 10.5194/bg-10-6279-2013

Bright RM, Zhao K, Jackson RB, Cherubini F. Quantifying surface albedo and other direct biogeophysical climate forcings of forestry activities. Glob Chang Biol. 2015; 21: 3246–3266. DOI: 10.1111/gcb.12951 [PubMed: 25914206]

Caicedo JPR, Verrelst J, Munoz-Mari J, Moreno J, Camps-Valls G. Toward a semiautomatic machine learning retrieval of biophysical parameters. IEEE J Sel Top Appl Earth Obs Remote Sens. 2014; 7: 1249–1259. DOI: 10.1109/JSTARS.2014.2298752

Chaturvedi RK, Singh S, Singh H, Raghubanshi AS. Assessment of allometric models for leaf area index estimation of Tectona grandis. Trop Plant Res. 2017; 4: 274–285. DOI: 10.22271/tpr.2017.v4.i2.037

Chianucci F, Macfarlane C, Pisek J, Cutini A, Casa R. Estimation of foliage clumping from the LAI-2000 Plant Canopy Analyzer: effect of view caps. Trees - Struct Funct. 2015; 29: 355–366. DOI: 10.1007/s00468-014-1115-x

Clevers JGPW, Kooistra L, van den Brande MMM. Using Sentinel-2 data for retrieving LAI and leaf and canopy chlorophyll content of a potato crop. Remote Sens. 2017; 9: 1–15. DOI: 10.3390/rs9050405

Croft H, Chen JM, Zhang Y. The applicability of empirical vegetation indices for determining leaf chlorophyll content over different leaf and canopy structures. Ecol Complex. 2014; 17: 119–130. DOI: 10.1016/j.ecocom.2013.11.005

Darvishzadeh R, Skidmore A, Atzberger C, van Wieren S. Estimation of vegetation LAI from hyperspectral reflectance data: effects of soil type and plant architecture. Int J Appl Earth Obs Geoinf. 2008a; 10: 358–373. DOI: 10.1016/j.jag.2008.02.005

Darvishzadeh R, Skidmore A, Schlerf M, Atzberger C. Inversion of a radiative transfer model for estimating vegetation LAI and chlorophyll in a heterogeneous grassland. Remote Sens Environ. 2008b; 112: 2592–2604. DOI: 10.1016/j.rse.2007.12.003

Delegido J, Verrelst J, Alonso L, Moreno J. Evaluation of sentinel-2 red-edge bands for empirical estimation of green LAI and chlorophyll content. Sensors. 2011; 11: 7063–7081. DOI: 10.3390/s110707063 [PubMed: 22164004]

Delegido J, Verrelst J, Rivera JP, Ruiz-Verdú A, Moreno J. Brown and green LAI mapping through spectral indices. Int J Appl Earth Obs Geoinf. 2015; 35: 350–358. DOI: 10.1016/j.jag.2014.10.001

Dorigo WA, Zurita-Milla R, de Wit AJW, Brazile J, Singh R, Schaepman ME. A review on reflective remote sensing and data assimilation techniques for enhanced agroecosystem modeling. Int J Appl Earth Obs Geoinf. 2007; 9: 165–193. DOI: 10.1016/j.jag.2006.05.003

European Space Agency. Sentinel Scientific Hub. 2016a.

European Space Agency. Sentinel Application Platform. 2016b.

European Space Agency. Sen2Cor. 2016c.

European Space Agency. Sentinel-2 User Handbook. 2015.

Feret JB, François C, Asner GP, Gitelson AA, Martin RE, Bidel LPR, Ustin SL, le Maire G, Jacquemoud S. PROSPECT-4 and 5: advances in the leaf optical properties model separating photosynthetic pigments. Remote Sens Environ. 2008; 112: 3030–3043. DOI: 10.1016/j.rse.2008.02.012

Gemmell F, Varjo J, Strandstrom M, Kuusk A. Comparison of measured boreal forest characteristics with estimates from TM data and limited ancillary information using reflectance model inversion. Remote Sens Environ. 2002; 81: 365–377. DOI: 10.1016/S0034-4257(02)00012-3

George R, Padalia H, Sinha SK, Kumar AS. Evaluation of the use of hyper-spectral vegetation indices for estimating mangrove leaf area index in Middle Andaman Island. India. Remote Sens Lett. 2018; 9: 1099–1108. DOI: 10.1080/2150704X.2018.1508910

Goel NS, Qin W. Influences of canopy architecture on relationships between various vegetation indices and LAI and FPAR: a computer simulation. Remote Sens Rev. 1994; 10: 309–347. DOI: 10.1080/02757259409532252

Goel NS, Thompson RL. A snapshot of canopy reflectance models and a universal nodel for the radiation regime. Remote Sens Rev. 2000; 18: 197–225. DOI: 10.1080/02757250009532390

Gong P, Pu R, Biging GS, Larrieu MR. Estimation of forest leaf area index using vegetation indices derived from Hyperion hyperspectral data. IEEE Trans Geosci Remote Sens. 2003; 41: 1355–1362. DOI: 10.1109/TGRS.2003.812910

Houborg R, Soegaard H, Boegh E. Combining vegetation index and model inversion methods for the extraction of key vegetation biophysical parameters using Terra and Aqua MODIS reflectance data. Remote Sens Environ. 2007; 106: 39–58. DOI: 10.1016/j.rse.2006.07.016

Huete A, Didan K, Miura H, Rodriguez EP, Gao X, Ferreira LF. Overview of the radiometric and biopyhsical performance of the MODIS vegetation indices. Remote Sens Environ. 2002; 83: 195–213.

Huete AR. A soil-adjusted vegetation index (SAVI). Bangladesh Med Res Counc Bull. 1988; 25: 295–309.

Immitzer M, Vuolo F, Atzberger C. First experience with Sentinel-2 data for crop and tree species classifications in central Europe. Remote Sens. 2016; 8 doi: 10.3390/rs8030166

Jacquemoud S. Inversion of the PROSPECT + SAIL canopy reflectance model from AVIRIS equivalent spectra: theoretical study. Remote Sens Environ. 1993; 44: 281–292. DOI: 10.1016/0034-4257(93)90022-P

Jacquemoud S, Baret F. PROSPECT: a model of leaf optical properties spectra. Remote Sens Environ. 1990; 34: 75–91. DOI: 10.1016/0034-4257(90)90100-Z

Jacquemoud S, Ustin SL, Verdebout J, Schmuck G, Andreoli G, Hosgood B. Estimating leaf biochemistry using the PROSPECT leaf optical properties model. Remote Sens Environ. 1996; 56: 194–202. DOI: 10.1016/0034-4257(95)00238-3

Jacquemoud S, Verhoef W, Baret F, Bacour C, Zarco-Tejada PJ, Asner GP, François C, Ustin SL. PROSPECT + SAIL models: A review of use for vegetation characterization. Remote Sens Environ. 2009; 113: S56–S66. DOI: 10.1016/j.rse.2008.01.026

Knyazikhin, Y, Glassy, J, Tian, Y. MODIS Leaf Area Index (LAI) And Fraction Of Photosynthetically Active Radiation Absorbed By Vegetation (FPAR) Product Algorithm Theoretical Basis Document. NASA; 1999. http://eospso.gsfc.nasa.gov/atbd/modistables.html

Li X, Mao F, Du H, Zhou G, Xu X, Han N, Sun S, Gao G, Chen L. Assimilating leaf area index of three typical types of subtropical forest in China from MODIS time series data based on the integrated ensemble Kalman filter and PROSAIL model. ISPRS J Photogramm Remote Sens. 2017; 126: 68–78. DOI: 10.1016/j.isprsjprs.2017.02.002

Liu, Lingling; Liang, L; Schwartz, MD; Donnelly, A; Wang, Z; Schaaf, CB; Liu, Liangyun. Evaluating the potential of MODIS satellite data to track temporal dynamics of autumn phenology in a temperate mixed forest. Remote Sens Environ. 2015; 160: 156–165. DOI: 10.1016/j.rse.2015.01.011

Lu X, Liu Z, Zhou Y, Liu Y, An S, Tang J. Comparison of phenology estimated from reflectance-based indices and solar-induced chlorophyll fluorescence (SIF) observations in a temperate forest using GPP-based phenology as the standard. Remote Sens. 2018; 10 doi: 10.3390/rs10060932

Main-Knorn M, Pflug B, Louis J, Debaecker V, Müller-Wilm U, Gascon F. Sen2Cor for Sentinel-2. Image Signal Process. Remote Sens. 2017; XXIII: 3. doi: 10.1117/12.2278218 1042704

Monsi M, Saeki T. Über den Lichtfaktor in den Pflanzengesellschaften und seine Bedeutung für die Stoffproduktion. Jpn J Bot. 1953; 14: 22–52. DOI: 10.1093/aob/mci052

Nemani RR, Keeling CD, Hashimoto H, Jolly WM, Piper SC, Tucker CJ, Myneni RB, Running SW. BIOFRAG research topic. Distribution. 2009; 300: 2007.

Padalia H, Sinha SK, Bhave V, Trivedi NK, Senthil Kumar A. Estimating canopy LAI and chlorophyll of tropical forest plantation (North India) using Sentinel-2 data. Adv Space Res. 2019; doi: 10.1016/j.asr.2019.09.023

Pearson, RL; Miller, LD. Remote mapping of standing crop biomass for estimation of the productivity of the shortgrass prairie, pawnee national grasslands, Colorado; Eighth International Symposium on Remote Sensing of Environment; 1972.

Pérez-Harguindeguy N, Díaz S, Garnier E, Lavorel S, Poorter H, Jaureguiberry P, Bret-Harte MS, Cornwell WK, Craine JM, Gurvich DE, Urcelay C, et al. New handbook for standardised measurement of plant functional traits worldwide. Aust J Bot. 2013; 61: 167–234. DOI: 10.1071/BT12225

Rasmussen CE, Williams CKI. Gaussian processes for machine learning. J Mach Learn Res. 2006; doi: 10.1142/S0129065704001899

Rivera JP, Verrelst J, Leonenko G, Moreno J. Multiple cost functions and regularization options for improved retrieval of leaf chlorophyll content and LAI through inversion of the PROSAIL model. Remote Sens. 2013; 5: 3280–3304. DOI: 10.3390/rs5073280

Ross, J. The Radiation Regime and Architecture of Plant Stands. Dr. W. Junk Publishers; The Hague: 1981.

Rouse, RWH; Haas, JAW; Deering, DW. Monitoring vegetation systems in the great plains with ERTS; Third Earth Resources Technology Satellite-1 Symposium-Volume I: Technical Presentations; 1974. 309–317. SP-351

Sehgal VK, Chakraborty D, Sahoo RN. Inversion of radiative transfer model for retrieval of wheat biophysical parameters from broadband reflectance measurements. Inf Process Agric. 2016; 3: 107–118. DOI: 10.1016/j.inpa.2016.04.001

Shukla UK, Bora DS. Geomorphology and sedimentology of Geomorphology and sedimentology of Piedmont zone, Ganga Plain. India Curr Sci. 2003; 84: 1034–1040.

Si Y, Schlerf M, Zurita-Milla R, Skidmore A, Wang T. Mapping spatio-temporal variation of grassland quantity and quality using MERIS data and the PROSAIL model. Remote Sens Environ. 2012; 121: 415–425. DOI: 10.1016/j.rse.2012.02.011

Spitters CJT. Separating the diffuse and direct component of global radiation and its implications for modeling canopy photosynthesis Part II. Calculation of canopy photosynthesis. Agric For Meteorol. 1986; 38: 231–242. DOI: 10.1016/0168-1923(86)90061-4

Tucker CJ. Red and photographic infrared linear combinations for monitoring vegetation. Remote Sens Environ. 1979; 8: 127–150. DOI: 10.1016/0034-4257(79)90013-0

Verrelst J, Camps-Valls G, Muñoz-Marí J, Rivera JP, Veroustraete F, Clevers JGPW, Moreno J. Optical remote sensing and the retrieval of terrestrial vegetation bio-geophysical properties - A review. ISPRS J Photogramm Remote Sens. 2015a; 108: 273–290. DOI: 10.1016/j.isprsjprs.2015.05.005

Verrelst J, Malenovský Z, van der Tol C, Camps-Valls G, Gastellu-Etchegorry JP, Lewis P, North P, Moreno J. Quantifying vegetation biophysical variables from imaging spectroscopy data: a review on retrieval methods. Surv Geophys. 2018; 40: 1–41. DOI: 10.1007/s10712-018-9478-y

Verrelst, J; Rivera, JP; Moreno, J. To Quantify Driving Variables of Leaf and; 9th EARSeL Imaging Spectroscopy Workshop; 2015b. 1–11.

Verrelst J, Rivera JP, Veroustraete F, Muñoz-Marí J, Clevers JGPW, Camps-Valls G, Moreno J. Experimental Sentinel-2 LAI estimation using parametric, nonparametric and physical retrieval methods - A comparison. ISPRS J Photogramm Remote Sens. 2015c; 108: 260–272. DOI: 10.1016/j.isprsjprs.2015.04.013

Vuolo F, Dini L, D'urso G. Assessment of LAI Retrieval Accuracy by Inverting a RT Model and a Simple Empirical Model With Multiangular and Hyperspectral CHRIS/PROBA Data From SPARC. Eur Sp Agency. 2005. 95–102.

Watson DJ. Comparative physiological studies on the growth of Field crops. Annals of Applied Biology. 1947; 1–37. DOI: 10.1111/j.1744-7348.1953.tb02364.x [PubMed: 20247586]

Weiss M, Baret F, Myneni RB, Pragnère A, Knyazikhin Y. Investigation of a model inversion technique to estimate canopy biophysical variables from spectral and directional reflectance data. Agronomie. 2000; 20: 3–22. DOI: 10.1051/agro:2000105

Woodgate W, Jones SD, Suarez L, Hill MJ, Armston JD, Wilkes P, Soto-Berelov M, Haywood A, Mellor A. Understanding the variability in ground-based methods for retrieving canopy openness, gap fraction, and leaf area index in diverse forest systems. Agric For Meteorol. 2015; 205: 83–95. DOI: 10.1016/j.agrformet.2015.02.012

Wu J, Chavana-Bryant C, Prohaska N, Serbin SP, Guan K, Albert LP, Yang X, van Leeuwen WJD, Garnello AJ, Martins G, Malhi Y, et al. Convergence in relationships between leaf traits, spectra and age across diverse canopy environments and two contrasting tropical forests. New Phytol. 2017; 214: 1033–1048. DOI: 10.1111/nph.14051 [PubMed: 27381054]

Wu L, Qin Q, Liu X, Ren H, Wang J, Zheng X, Ye X, Sun Y. Spatial upscaling correction for leaf area index based on the fractal theory. Remote Sens. 2016; 8 doi: 10.3390/rs8030197

Wulder MA, Masek JG, Cohen WB, Loveland TR, Woodcock CE. Opening the archive: how free data has enabled the science and monitoring promise of Landsat. Remote Sens Environ. 2012; 122: 2–10. DOI: 10.1016/j.rse.2012.01.010

Yang G, Zhao C, Liu Q, Huang W, Wang J. Inversion of a Radiative Transfer Model for Estimating. 2011; 49: 988–1000.

Yang W, Huang D, Tan B, Stroeve JC, Shabanov NV, Knyazikhin Y, Nemani RR, Myneni RB. Analysis of leaf area index and fraction of PAR absorbed by vegetation products from the terra MODIS sensor: 2000-2005. IEEE Trans Geosci Remote Sens. 2006; 44: 1829–1841. DOI: 10.1109/TGRS.2006.871214

Yang X, Tang J, Mustard JF, Wu J, Zhao K, Serbin S, Lee JE. Seasonal variability of multiple leaf traits captured by leaf spectroscopy at two temperate deciduous forests. Remote Sens Environ. 2016; 179: 1–12. DOI: 10.1016/j.rse.2016.03.026

Zhou L, Tian Y, Myneni RB, Ciais P, Saatchi S, Liu YY, Piao S, Chen H, Vermote EF, Song C, Hwang T. Widespread decline of Congo rainforest greenness in the past decade. Nature. 2014; 508: 86–90. DOI: 10.1038/nature13265

Europe PMC Funders Author Manuscripts

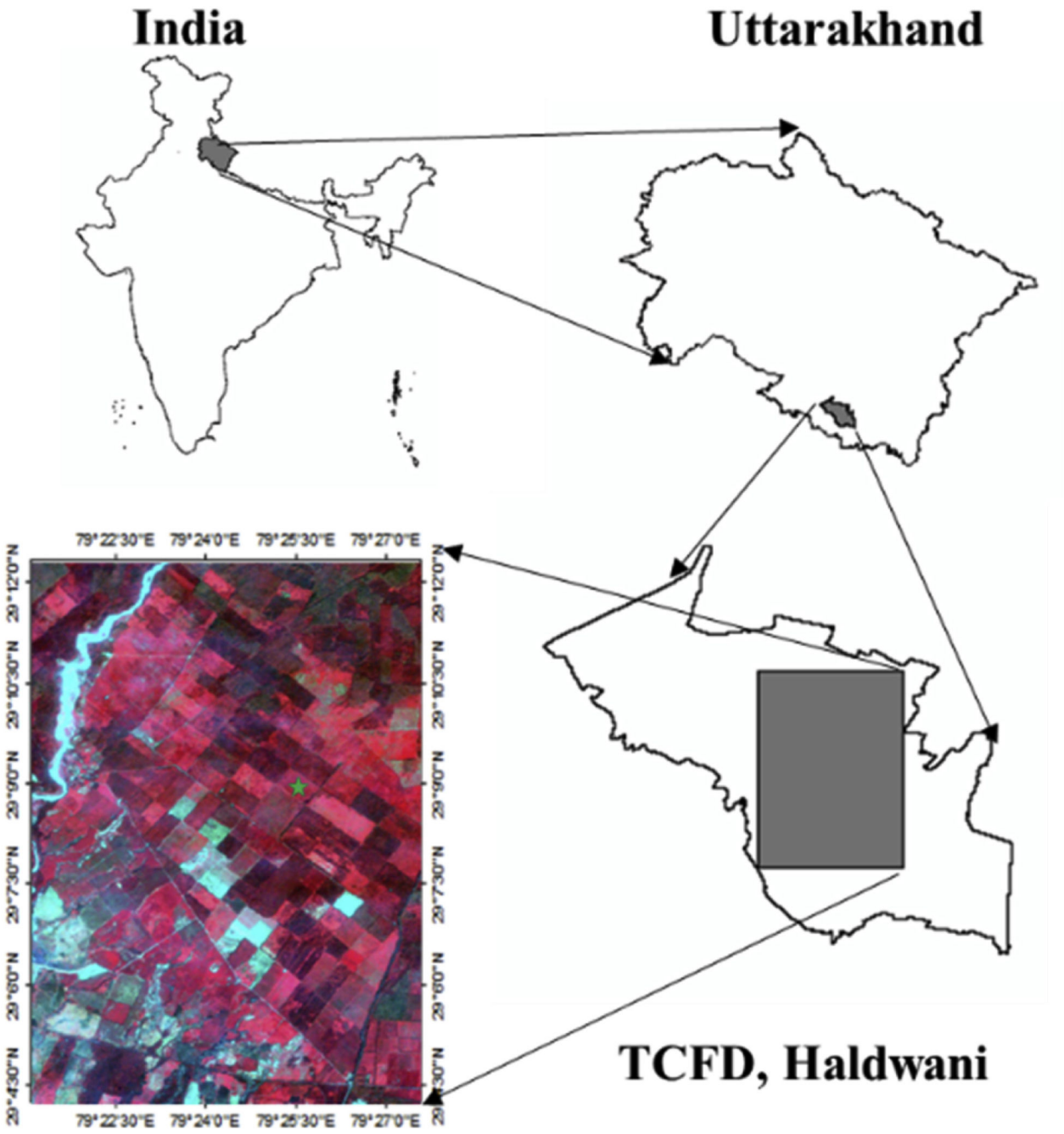

Fig. 1. Location map of the study area.

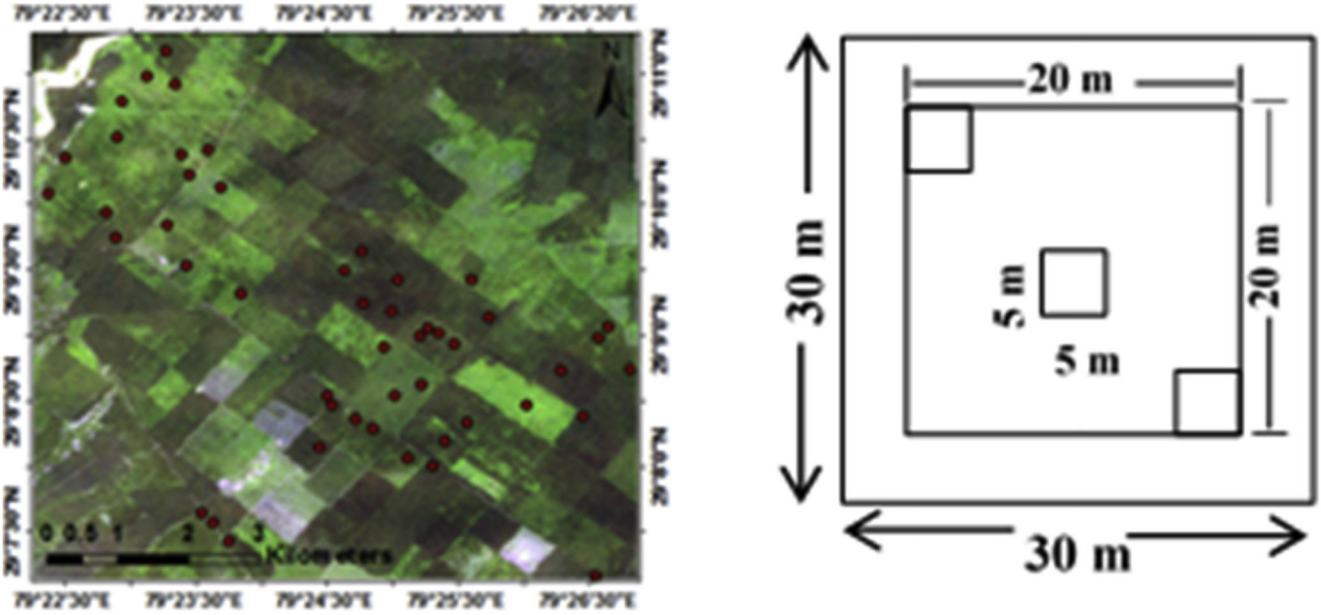

Fig. 2.
Field sampling design (a) EEUs superimposed on Sentinel-2 Natural color composite (b) EEU design.

Europe PMC Funders Author Manuscripts

Europe PMC Funders Author Manuscripts

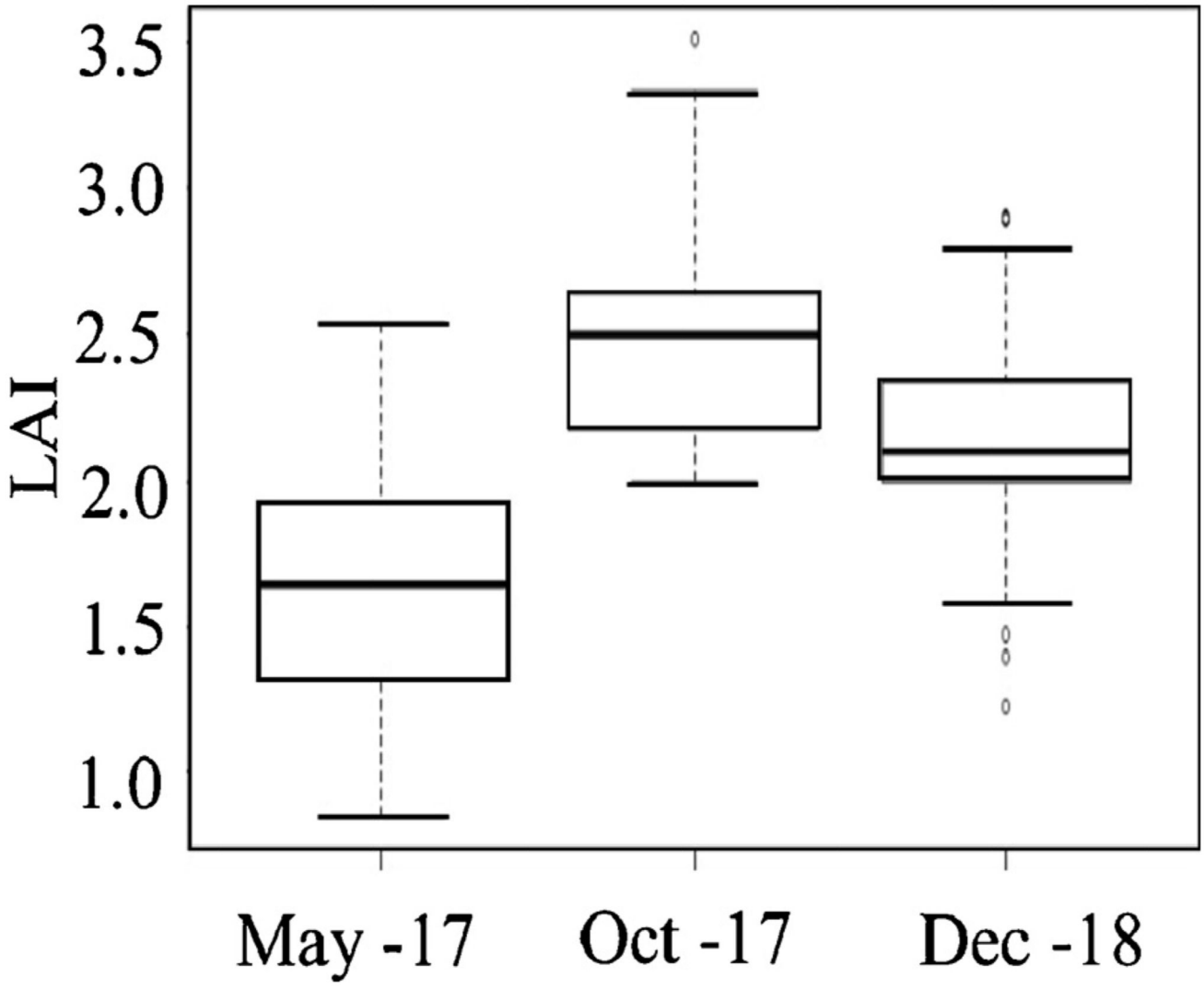

Fig. 3.
LAI box plots showing seasonal variability in LAI (mean ± standard deviation).

Europe PMC Funders Author Manuscripts

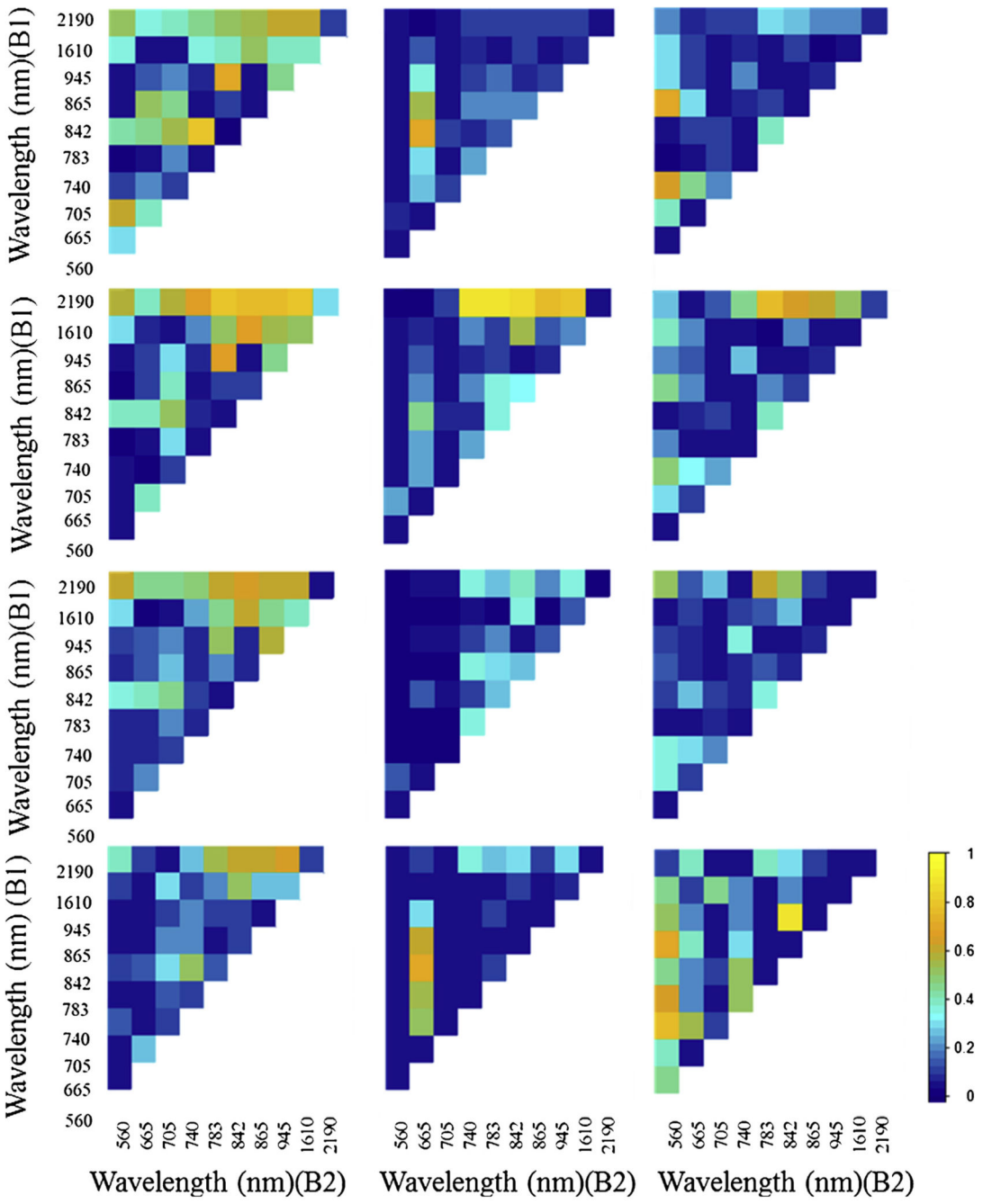

Fig. 4.

2D correlation matrix of SR, NDVI, SAVI, and NLI (linear) (top to bottom) with field LAI for May, October and December month (left to right).

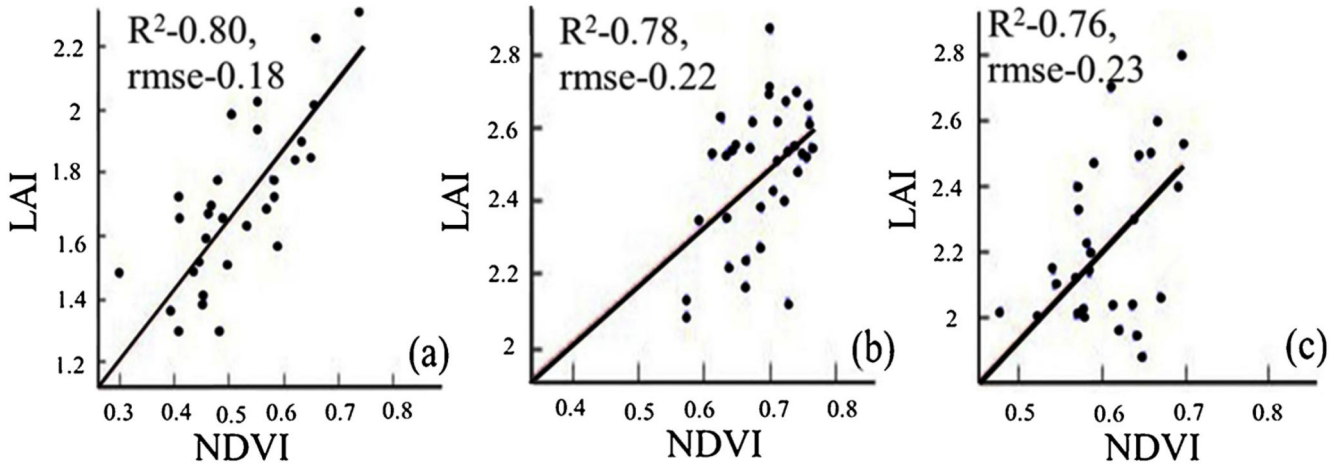

Fig. 5.

LAI relationship with NDVI of (a)May, (b) October, (c)December, and (d) residual errors for May, (e) October, (f) December.

Europe PMC Funders Author Manuscripts

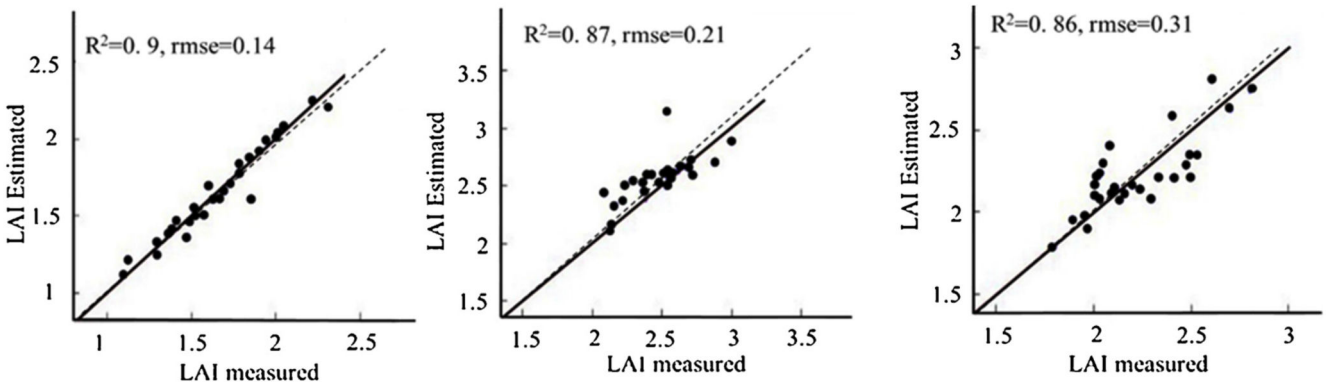

Fig. 6.

Estimation of LAI using MLRA-GPR for May 2018, October 2017 and December 2017 (left to right).

Europe PMC Funders Author Manuscripts

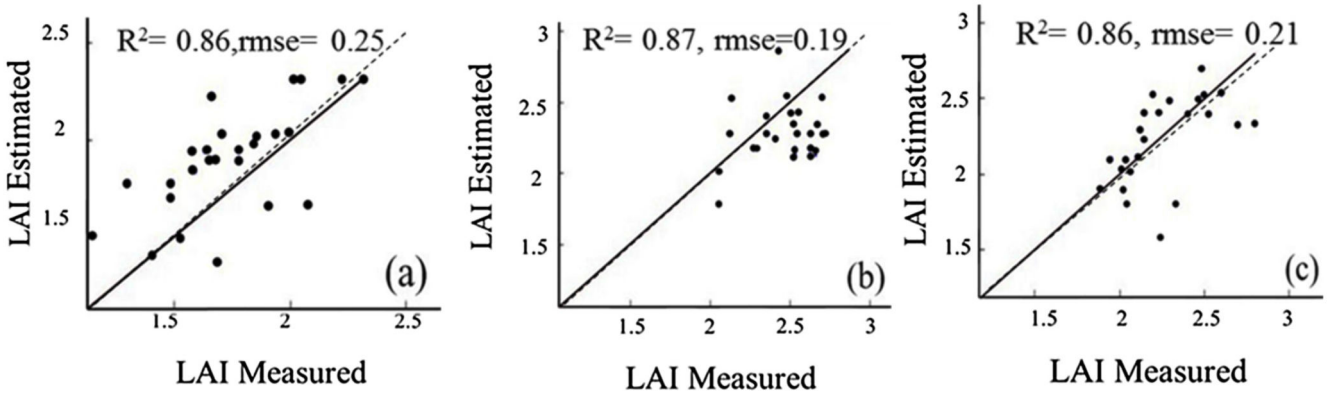

Fig. 7.
LUT results for (a) May 2018, (b) October 2017, (c) December 2017.

Europe PMC Funders Author Manuscripts

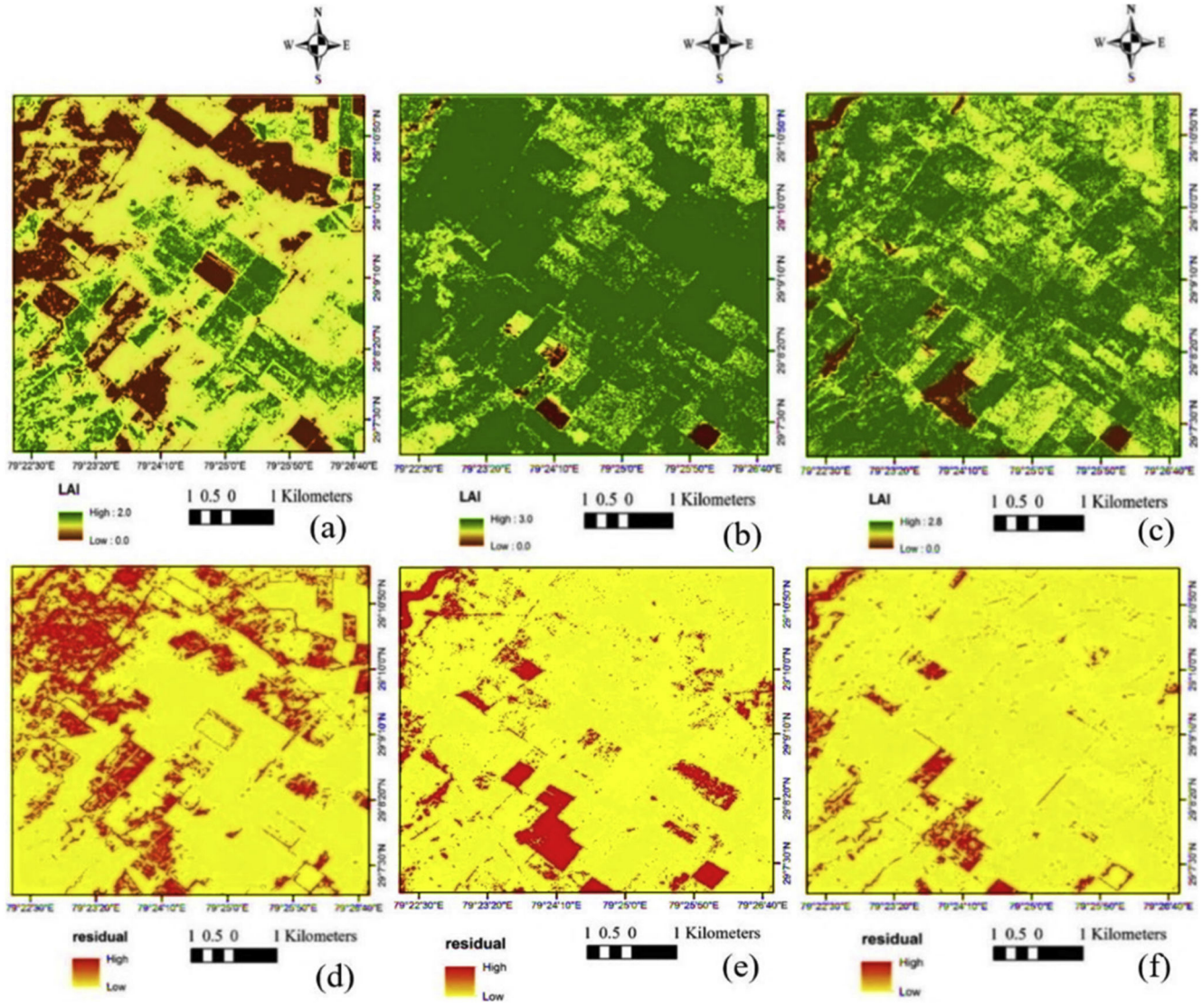

Fig. 8.

LAI maps for (a) May (b) October (c) December (d) and residual error maps of May (e), October (f) December.

Europe PMC Funders Author Manuscripts

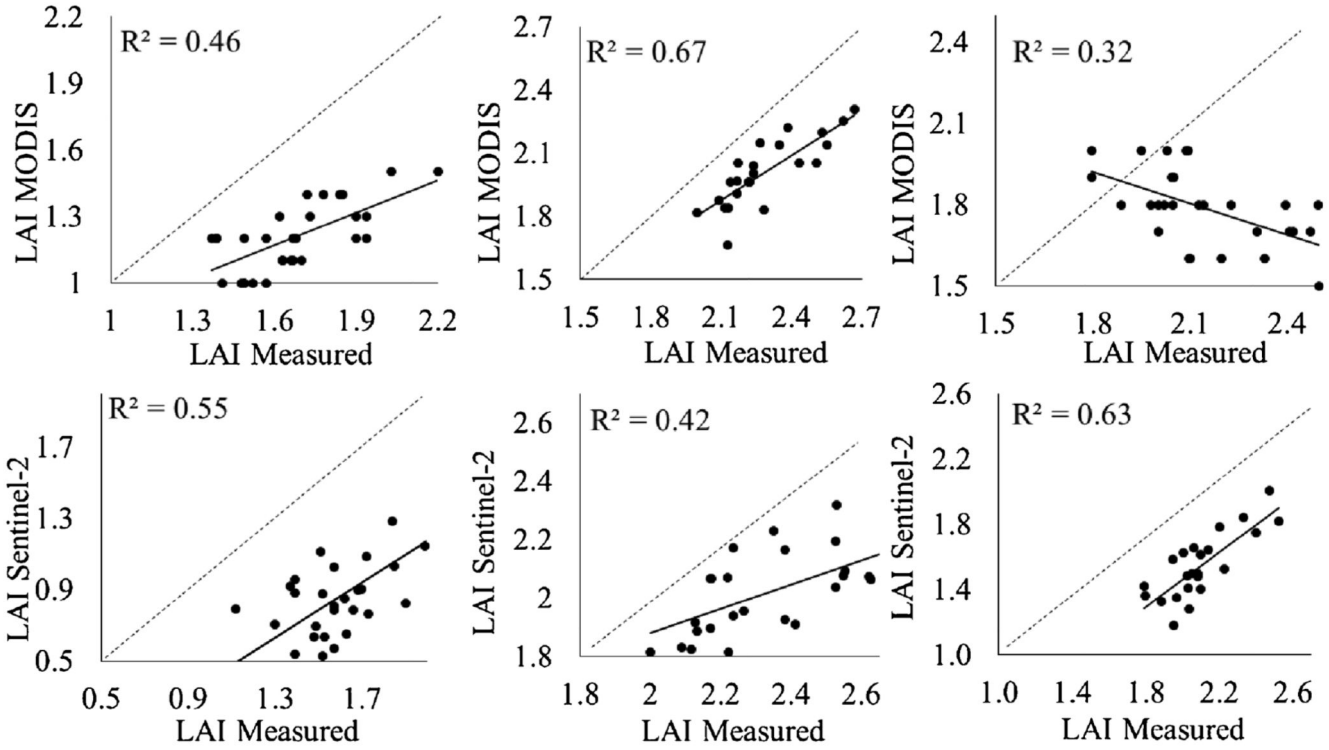

Fig. 9.

Relationship of measured LAI with global MODIS LAI products (Upper) and Sentinel-2 LAI (lower) for May, October and December month (left to right).

Europe PMC Funders Author Manuscripts

Europe PMC Funders Author Manuscripts

Table 1

List of parameters and their ranges used in PROSAIL reflectance modeling.

Parameter	Symbol	Unit	Growing Season Range	Peak Season Range	Senescence Season Range
Leaf structural index[a]	N	–	1.5–2.5	1.5–2.5	1.5–2.5
Leaf chlorophyll content	Cab	mg/cm^2	0–58	0–65	0–63
Leaf dry matter content	C_m	g/cm^2	0.012–0.03	0.012–0.03	0.012–0.03
Equivalent water thickness	C_w	g/cm^2	0.03-0.05	0.03–0.05	0.03–0.048
Leaf area index	LAI	$m^2\ m^{-2}$	0-2.2	0–2.8	0–3.3
Soil brightness coefficient[a]	Scale	–	0.2 -1	0.2–1	0.2–1
Average leaf angle	ALA	°	20 -50	20–50	17–50
Hot spot parameter[a]	hot	$m\ m^{-1}$	0.01	0.01	0.01
Diffuse radiation (%)	skyl	Fraction	10-23	10–23	10–23
Solar zenith angle	φ^v	°	46	47	45
View azimuth angle	φ^v	°	Fixed	Fixed	Fixed
View observer angle	φ^v	°	Fixed	Fixed	Fixed

[a]Ranges were constrained based on literature.

Table 2
VIs, their formulation and importance for LAI estimation.

VIs	Formula	Importance for LAI estimation
SR [a]	$p\lambda 1/p\lambda 2$ *	Index used to determine vegetation vigour.
NDVI [b]	$(\rho\lambda - \rho\lambda 2)/(\rho\lambda 1 + \rho\lambda 2)$ *	Awidely used and much-studied index that helps in relating the visual change in pigment concentration (Rouse et al., 1974; Tucker, 1979; Baret and Guyou, 1991)
SAVI [c]	$\frac{(p\lambda - p\lambda 2)}{(p\lambda 1 + p\lambda 2 + L)}(1 + L)$ * L = 0.5 is the correction factor.	SAVI reduces background soil noise problems for a wide range of LAI (Huete, 1988).
NLI [d]	$(\rho\lambda 1^2 - \rho\lambda 2)/(\rho\lambda 1^2 + \rho\lambda 2)$*	NLI considers the relationship between VIs and biophysical parameters by linearizing the non-linear relationship (Goel and Qin, 1994).

[a] Simple Ratio (Pearson and Miller, 1972),

[b] Normalized Difference Vegetation Index,

[c] Soil Adjusted Vegetation Index,

[d] Non-Linear Vegetation Index,

* ρ is the apparent reflectance, λ1 and λ2 are the wavelengths.

Europe PMC Funders Author Manuscripts

Table 3

Seasonal performance of different retrieval methods.

Retrieval methods	May		October		December	
	R^2	RMSE	R^2	RMSE	R^2	RMSE
Parametric Regression Model (NDVI)	0.80	0.18	0.78	0.22	0.76	0.23
Non-Parametric Regression Model (MLRA-GPR)	**0.90**	0.14	**0.87**	0.21	**0.86**	0.31
Physically based LUT Inversion methods	0.86	0.25	**0.87**	**0.19**	**0.86**	**0.21**